Available online at www.sciencedirect.com
ScienceDirect
Ceramics International 36 (2010) 821–826
CERAMICS INTERNATIONAL
www.elsevier.com/locate/ceramint

Short communication

Effect of Al_2O_3 content on $BaO–Al_2O_3–B_2O_3–SiO_2$ glass sealant for solid oxide fuel cell

Tao Sun [a], Hanning Xiao [a,b,*], Wenming Guo [a], Xiucheng Hong [b]

[a] College of Materials Science and Engineering, Hunan University, Changsha 410082, China
[b] College of Physics and Electronic Science, Changsha University of Science & Technology, Changsha 410076, China

Received 20 July 2009; received in revised form 29 July 2009; accepted 22 September 2009
Available online 29 October 2009

Abstract

The glass structure, wetting behavior and crystallization of $BaO–Al_2O_3–B_2O_3–SiO_2$ system glass containing 2–10 mol% Al_2O_3 were investigated. The introduction of Al_2O_3 caused the conversion of $[BO_3]$ units and $[BO_4]$ units to each other and it played as glass network former when the content was up to 10 mol%, accompanied by $[BO_4] \rightarrow [BO_3]$. The stability of the glass improved first and then decreased as Al_2O_3 increased from 2 to 10 mol%, the glass with 5 mol% Al_2O_3 being the most stable one. The wetting behavior of the glasses indicates that excess Al_2O_3 leads to high sealing temperature. The glass containing 5 mol% Al_2O_3 characterized by a lower sealing temperature is suitable for SOFC sealing. Al_2O_3 improves the crystallization temperature of the glass. The crystal phases in the reheated glasses are mainly composed of $Ba_2Si_3O_8$, $BaSiO_3$, BaB_2O_4 and $BaAl_2Si_2O_8$. Al_2O_3 helps the crystallization of $BaSiO_3$ and $BaAl_2Si_2O_8$.

Keywords: $BaO–Al_2O_3–B_2O_3–SiO_2$ glass; SOFC sealant; Glass structure; Wetting behavior

1. Introduction

Solid oxide fuel cells (SOFCs) are energy conversion devices which produce electricity by the electrochemical reaction between fuel and an oxidant [1]. A key problem in the fabrication of planar SOFCs is the sealing of the electrolyte or the ceramic anode with the metallic interconnect in order to achieve a hermetic and stable cell [2]. The sealants must be stable in a wide range of oxygen partial pressure (air and fuel) and be chemically compatible with other fuel cell components [3–5]. The sealing material must provide tightness to avoid the leakage of reactant gases and meet a series of thermal, mechanical and chemical requirements. By carefully choosing the glass composition, glass–ceramics is considered as an ideal sealant since it can meet most of the requirements [6–10]. One of the major advantages of glass–ceramic sealants is that the chemical compositions of the glass can be tailored so as to control some important physical properties such as the coefficient of thermal expansion (CTE), viscosity, etc.

The $BaO–Al_2O_3–B_2O_3–SiO_2$ glass system is one of the potential systems for sealing SOFC with ZrO_2 electrolyte because of its suitable thermomechanical properties. In this system, Al_2O_3 is an important component of the glass system for SOFC sealants. In tetrahedral coordination it replaces silicon in the glass network, but at larger concentrations acts as a network modifier [11]. For this dual role, Al_2O_3 may inhibit [4] or enhance crystallization [12]. Al_2O_3 has also been reported to inhibit cristobalite formation [13], which can cause cracking. Meinhardt et al. synthesized a barium aluminosilicate glass–ceramic sealant containing 2.5–5 mol% Al_2O_3, in which Al_2O_3 was used to adjust viscosity by controlling the rate of crystallization [14].

The influence of glass components on the sealing behavior of SOFCs has been the object of a number of investigations [15–17]. However the role of Al_2O_3 in the glass sealants has been poorly uninvestigated. In the present work, a series of glasses were prepared by the melting–quenching method, and the effects of Al_2O_3 on the glass structure, wetting behavior and crystallization were discussed.

* Corresponding author at: College of Materials Science and Engineering, Hunan University, Changsha 410082, China. Tel.: +86 731 888822269; fax: +86 731 882617678.
E-mail address: hnxiao@hnu.cn (H. Xiao).

0272-8842/$36.00
doi:10.1016/j.ceramint.2009.09.045

Table 1
Glass compositions in present work.

Glass ID	Chemical composition (mol%)			
	BaO	B_2O_3	SiO_2	Al_2O_3
A0	40	20	40	0
A1	40	19.3	38.7	2
A2	40	18.3	36.7	5
A3	40	16.7	33.3	10

2. Experimental procedure

2.1. Glass preparation

Chemical compositions of the glasses are listed in Table 1. The composition 40BaO–20B_2O_3–40SiO_2 (mol%) was used as basic glass, and different amounts of Al_2O_3 (2–10 mol%) were introduced to replace SiO_2 and B_2O_3 in the basic glass according to the same SiO_2/B_2O_3 ratio. Reagent-grade $BaCO_3$, H_3BO_3, SiO_2, and Al_2O_3, >99 wt% purity were chosen as the starting materials. After uniform mixing, the batches were melted at 1400–1500 °C for 1 h. The clarified molten glass was quenched in a graphite mould, then transferred to a furnace for annealing at 550 °C for 1 h before cooling down to room temperature. The bulk glasses were machined into bar specimen (5 mm × 5 mm × 25 mm) for CTE measurement, and the others were milled into powders (38–45 μm) for the IR, DSC, XRD and wetting tests.

2.2. Testing and characterization

The infrared spectra of the glasses were recorded at room temperature using the KBr disc technique. A Rayleigh WQF-410 FTIR spectrometer was used to obtain the spectra in the wave number range between 400 and 2000 cm^{-1} with a resolution of 2 cm^{-1}. Characteristic temperatures (glass transition temperature T_g, onset and maximum crystallization temperature T_x and T_p, melting temperature T_m) were determined by differential scanning calorimetry (DSC) using a NETZSCH STA 449PC calorimeter at a heating rate of 10 °C min^{-1}. The CTE of the glasses was measured using a NETZSCH DIL 402PC dilatometer with a heating rate of 5 °C min^{-1}. Crystal phases of reheated samples were analyzed by X-ray diffraction (XRD) using CuKα radiation with a Rigaku D/Max 2200PC equipment.

Wetting experiments were conducted in a furnace with a visualization window, in which the heated specimen could be observed. A camera was used to record the melting and wetting behavior of the glass (in pellet form with size of Φ 8 mm × 10 mm) on an YSZ substrate. The YSZ plate was prepared using an 8 mol% Y_2O_3–ZrO_2 powder compact sintered at 1500 °C, then polished with diamond paste to obtain a smooth surface.

3. Results and discussion

3.1. Glass structure

Fig. 1 shows the infrared absorption spectra of the BaO–Al_2O_3–B_2O_3–SiO_2 glasses. The IR spectra of the Al_2O_3 free glass A0 showed six main bands. The band at about 471 cm^{-1} is due to Si–O–Si asymmetric bending vibration and the small shoulder located at 724 cm^{-1} is attributed to bending vibration of B–O–B in [BO_3] triangles [18–21]. The main intense band located at 850–1100 cm^{-1} represents a superposition of two bands situated close to each other at about 925 and 1012 cm^{-1}, the absorption peak near 925 cm^{-1} is assigned to the stretching vibration of [BO_4] tetrahedral and the band near 1012 cm^{-1} is due to the combined stretching vibrations of Si–O–Si and B–O–B network of tetrahedral structural units [20–24]. The shoulder at 1220 cm^{-1} is due to the stretching vibration of the boroxol ring and the band centered at 1402 cm^{-1} is attributed to the B–O stretching vibration of [BO_3] triangles (characteristic for the [BO_3] group) [21,22,25].

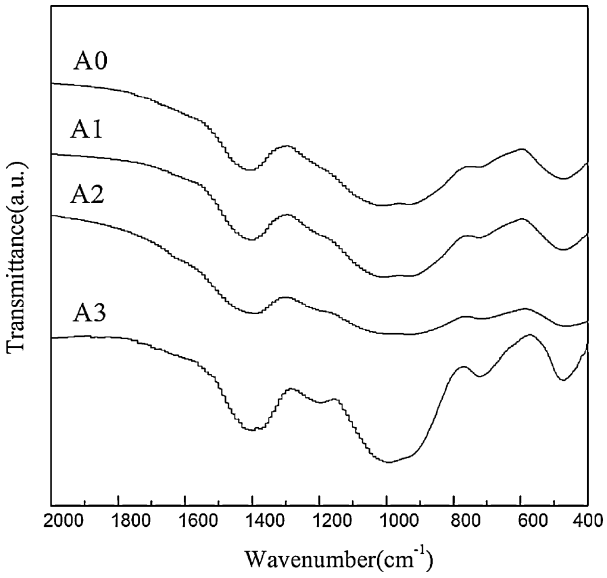

Fig. 1. Infrared absorbance spectra of glass samples.

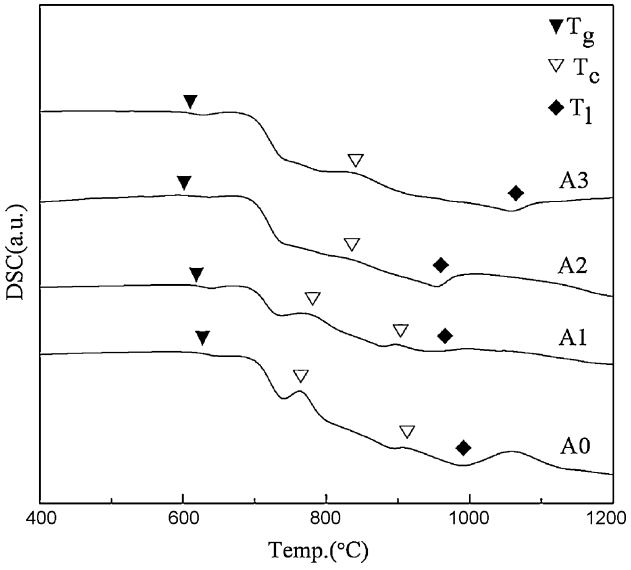

Fig. 2. DSC curves of glass samples.

Table 2
Thermal properties and CTE of glass samples.

Glass no.	T_g (°C)	T_x (°C)	T_{p1} (°C)[a]	T_{p2} (°C)[a]	T_l (°C)	ΔT (°C)	K_{gl}	CTE ($\times 10^{-6}$ °C^{-1})
A0	622.0	740.9	762.7	906.9	991.0	118.9	0.48	10.83
A1	617.5	741.7	765.4	896.1	965.2	120.3	0.53	10.57
A2	601.8	802.4	830.0	–	953.7	200.6	1.33	10.67
A3	605.8	795.0	838.2	–	1058.3	189.2	0.72	10.34

[a] T_{p1} is the first crystallization exothermic peak temperature and T_{p2} is the second one.

The introduction of Al_2O_3 caused a little change to the glass structure (Fig. 1). The bands centered at 992–1012 cm^{-1} are the main intense band inselective of the Al_2O_3 amount. At Al_2O_3 is ≤5 mol%, the intensity of the band located at 724 cm^{-1} decreased, while it strengthened when Al_2O_3 increased to 10 mol%. The absorption band of [AlO_4] is located in the same position as the borate groups [20,22], so it is difficult to identify the band at 724 cm^{-1} belonging to [BO_3] group or the combination of [BO_3] and [AlO_4] group. The conversion between [BO_3] units and [BO_4] units can be confirmed by the change of the band at 925 cm^{-1} (characteristic for the [BO_4] group) and the band at 1402 cm^{-1} (characteristic for the [BO_3] group). The equilibrium between [BO_3] and [BO_4] groups is mainly depending on the Al_2O_3 content [24,26]. The increase of [BO_3] and decrease of [BO_4] groups in A3 glass indicate the content of Al_2O_3 to be sufficient to satisfy the formation of maximum amount of [BO_4] groups. This clearly suggests that Al_2O_3 is acting as network former in A3 glass. The vibration band of boroxol ring located at 1220 cm^{-1} turned clearer with the increase of Al_2O_3 which indicates that Al_2O_3 is helpful to the formation of boroxol ring.

3.2. Glass thermal stability

A parameter usually employed to estimate the glass stability is the thermal stability, which is defined by $\Delta T = T_x - T_g$ [27]. Another parameter introduced by Hruby [28,29] is the glass forming ability (K_{gl}) which is defined by the relation:

$$K_{gl} = \frac{T_x - T_g}{T_m - T_x} \quad (1)$$

Both an increasing $\Delta T = T_x - T_g$ or a decreasing temperature interval $T_m - T_x$ indicate an increasing glass stability and a lower tendency toward crystallization.

Fig. 2 shows the DSC curves of glass samples. Glasses A0 and A1 show two exothermic peaks, but only one in the other two glasses, the exothermic peak of both being very weak. The characteristic temperatures and glass stability parameters are listed in Table 2 whereas the composition dependence of T_g, T_x and T_l is shown in Fig. 3. The curves of K_{gl} and ΔT vs. Al_2O_3 content are shown in Figs. 4 and 5, respectively. It can be seen that an increase of Al_2O_3 (≤5 mol%) leads to a decrease of T_g and an increase of ΔT and K_{gl}. This means the introduction of Al_2O_3 to the glass system helps to improve glass stability and to decrease the trend to crystallization. When the content of Al_2O_3 increased to 10 mol%, T_g increased and ΔT and K_{gl} decreased indicating that a further increase of Al_2O_3 caused a decrease of the thermal stability of the glass.

The CTE values of glasses are also listed in Table 2 and the CTE vs. Al_2O_3 content is shown in Fig. 6. All the CTE of the glasses are in the range (9–12 × 10^{-6}) °C^{-1} which can match with other components of SOFC [30]. With the Al_2O_3 increase, CTE increased first and then decreased.

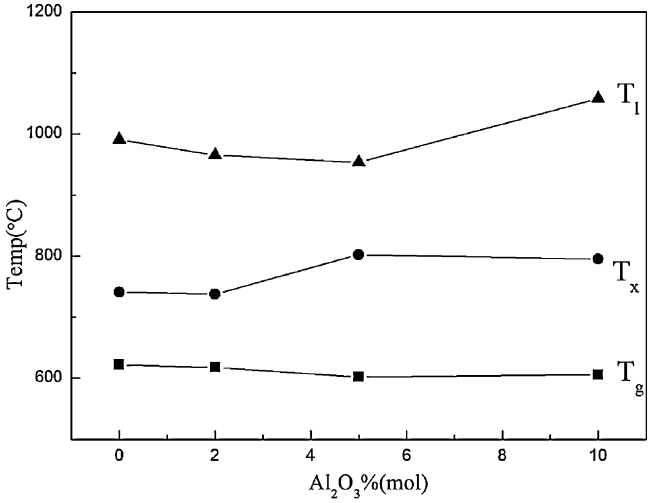

Fig. 3. T_g, T_x and T_l vs. Al_2O_3 content.

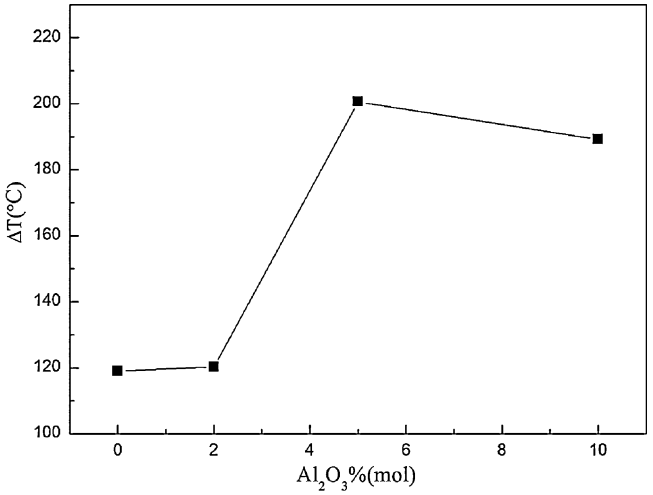

Fig. 4. ΔT vs. Al_2O_3 content.

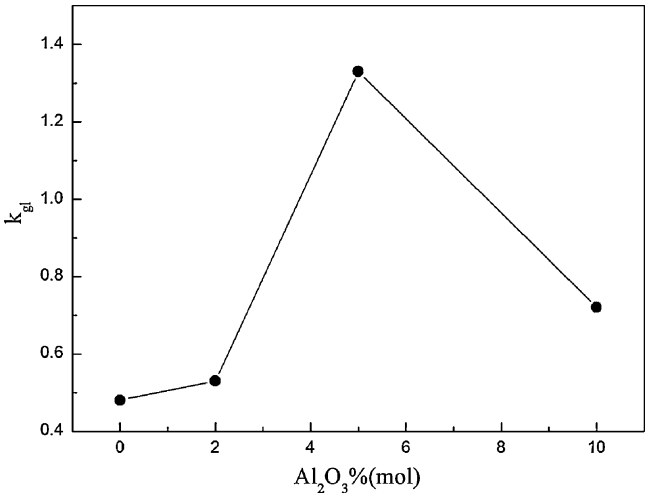

Fig. 5. K_{gl} vs. Al_2O_3 content.

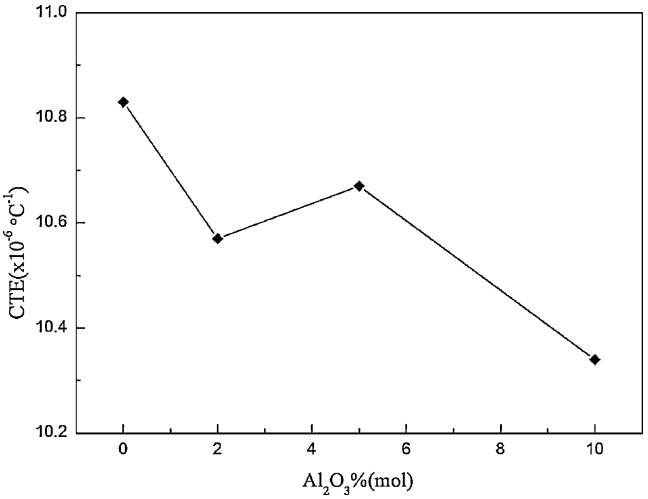

Fig. 6. CTE vs. Al_2O_3 content.

3.3. Bonding characteristics and wetting behavior to YSZ

The bonding characteristics and wetting behavior of the glass to YSZ were investigated by observing the shape change of the glass pellet on the YSZ plate with increasing temperature. Fig. 7 depicts the deformation of A2 glass pellet on YSZ plate with increasing temperature. The glass A2 shows well wetting behavior at about 940 °C with a contact angle near 45°. The variation of the contact angle of glasses with the temperature is shown in Fig. 8. All glasses can bond and wet YSZ if the temperature is high enough. Glass A0 (Al_2O_3 free) has a sealing temperature (the temperature where the contact angle near 45° has a suitable viscosity to seal) higher than 1000 °C. This reduces to 940 °C when the content of Al_2O_3 increased to 5 mol%, just in the range of 900–950 °C (temperature suitable for SOFC sealing) [15]. At increased Al_2O_3 content, the sealing temperature improved sharp to about 1040 °C.

3.4. Crystallization behavior

Fig. 9 shows the XRD patterns of the glasses heat-treated at 800 °C for 10 h. Barium borate silicate ($Ba_3B_6Si_2O_{16}$) is the primary phase along with a small amount of Barium silicate ($Ba_2Si_3O_8$) in glass A0 (Al_2O_3 free). But in the glass A1 containing 2 mol% Al_2O_3, $Ba_2Si_3O_8$ coexisting with Barium borate (BaB_2O_4) is the main crystal phase after the long time heat treatment, and at weak peaks hexacelsian ($BaAl_2Si_2O_8$) also appeared. Increased the Al_2O_3 content to 5 mol%, no new phase was detected in the reheated glass A2 except that peaks of BaB_2O_4 and $BaAl_2Si_2O_8$ strengthened. The XRD pattern of the glass A3 with 10 mol% Al_2O_3 revealed that no $Ba_2Si_3O_8$ but $BaSiO_3$ was detected, and $BaSiO_3$ is the predominant phase. Compared with glass A2, the $BaAl_2Si_2O_8$ phase in glass A3 increased a lot, while the BaB_2O_4 phase decreased.

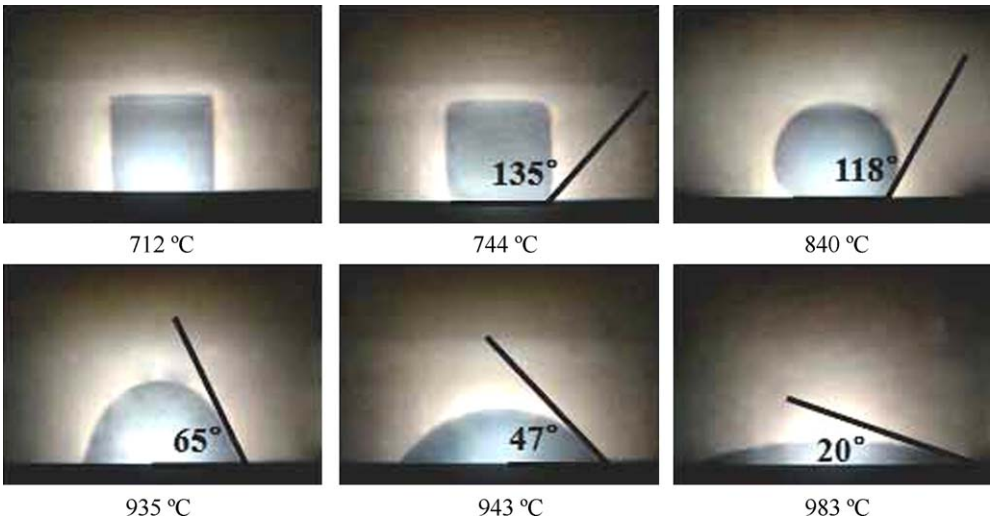

Fig. 7. Shape change of A2 glass pellet on 8YSZ substrate as a function of temperature (heating rate of 10 °C min^{-1}).

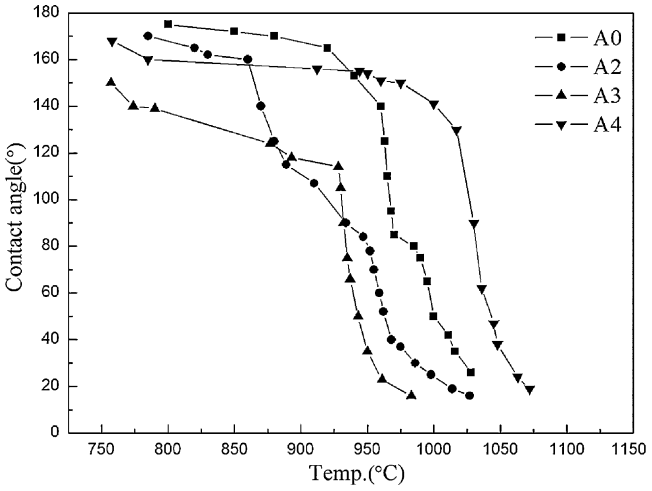

Fig. 8. Contact angle of the glass pellets on 8YSZ substrate as a function of the heating temperature (heating rate of 10 °C min^{-1}).

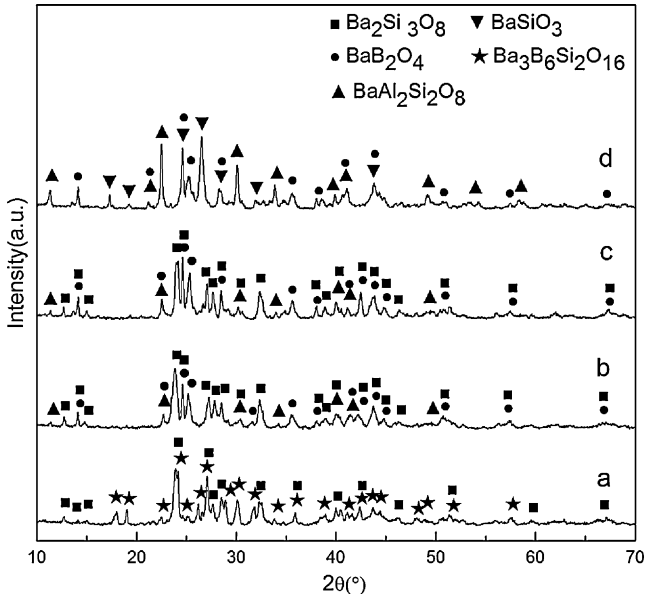

Fig. 9. XRD patterns of glasses heat-treated at 800 °C for 10 h. (a) A0, (b) A1, (c) A2, and (d) A3.

4. Conclusion

A glass was prepared from the $BaO–Al_2O_3–B_2O_3–SiO_2$ by the melting–quenching method. The effects of Al_2O_3 on the glass structure, wetting behavior and crystallization were investigated. The introduction of Al_2O_3 caused the conversion of $[BO_3]$ units and $[BO_4]$ units to each other. Al_2O_3 started behaving as glass network former when the addition of Al_2O_3 was up to 10 mol%. The stability of the glass increased first and then decreased as Al_2O_3 increased from 2 to 10 mol%, the 5 mol% Al_2O_3 glass being the most stable. The wetting behavior of the glasses indicates that excess Al_2O_3 leads to high sealing temperature. The 5 mol% Al_2O_3 glass shows a lower sealing temperature suitable for SOFC sealing. The introduction of Al_2O_3 increases the crystallization temperature of the glass. The crystal phases in the reheated glasses mainly include $Ba_2Si_3O_8$, $BaSiO_3$, BaB_2O_4 and $BaAl_2Si_2O_8$. Al_2O_3 addition helps the crystallization of $BaSiO_3$ and $BaAl_2Si_2O_8$.

References

[1] B.C.H. Steele, A. Heinzel, Materials for fuel-cell technologies, Nature 414 (2001) 345–352.
[2] M.J. Pascual, A. Guillet, A. Durán, Optimization of glass–ceramic sealant compositions in the system $MgO–BaO–SiO_2$ for solid oxide fuel cells (SOFC), J. Power Sources 169 (2007) 40–46.
[3] W. Jeffrey, Fergus, Sealants for solid oxide fuel cells, J. Power Sources 147 (2005) 46–57.
[4] K.L. Ley, M. Krumpelt, R. Kumar, J.H. Meiser, I. Bloom, Glass–ceramic sealants for solid oxide fuel cells: Part I. Physical properties, J. Mater. Res. 11 (1996) 1489–1493.
[5] C. Lara, M.J. Pascual, M.O. Prado, A. Durán, Sintering of glasses in the system $RO–Al_2O_3–BaO–SiO_2$ (R = Ca, Mg, Zn) studied by hot-stage microscopy, Solid State Ionics 170 (2004) 201–208.
[6] C. Lara, M.J. Pascual, A. Durán, Glass-forming ability, sinterability and thermal properties in the systems $RO–BaO–SiO_2$ (R = Mg Zn), J. Non-Cryst. Solids 348 (2004) 149–155.
[7] N.P. Bansal, E.A. Gamble, Crystallization kinetics of a solid oxide fuel cell seal glass by differential thermal analysis, J. Power Sources 47 (2005) 107–115.
[8] Z. Yang, Meinhardt, D. Kerry, J.W. Stevenson, Chemical compatibility of barium–calcium–aluminosilicate-based sealing glasses with the ferritic stainless steel interconnect in SOFCs, J. Electrochem. Soc. 150 (2003) A1095–A1101.
[9] P. Batfalsky, V.A.C. Haanappel, J. Malzbender, N.H. Menzler, V. Shemet, I.C. Vinke, R.W. Steinbrech, Chemical interaction between glass–ceramic sealants and interconnect steels in SOFC stacks, J. Power Sources 155 (2006) 128–137.
[10] M. Brochu, B.D. Gauntt, R. Shah, G. Miyake, R.E. Loehman, Comparison between barium and strontium–glass composites for sealing SOFCs, J. Eur. Ceram. Soc. 26 (2006) 3307–3313.
[11] P.W. Micmillan, Glass Ceramic, 2nd ed., Academic Press, London, 1979.
[12] N. Lahl, K. Singh, L. Singheiser, K. Hilpert, D. Bahadur, Crystallisation kinetics in $AO–Al_2O_3–SiO_2–B_2O_3$ glasses (A = Ba, Ca, Mg), J. Mater. Sci. 35 (2000) 3089–3096.
[13] N. Lahl, D. Bahadur, K. Singh, L. Singheiser, K. Hilpert, Chemical interactions between aluminosilicate base sealants and the components on the anode side of solid oxide fuel cells, J. Electrochem. Soc. 149 (2002) A607–A614.
[14] K.D. Meinhardt, D.-S. Kim, Y.-S. Chou, K.S. Weil, Synthesis and properties of a barium aluminosilicate solid oxide fuel cell glass–ceramic sealant, J. Power Sources 182 (2008) 188–196.
[15] S.-B. Sohn, S.-Y. Choi, G.-H. Kim, H.-S. Song, G.-D. Kim, Stable sealing glass for planar solid oxide fuel cell, J. Non-Cryst. Solids 297 (2002) 103–112.
[16] Ashutosh Goel, U. Dilshat, Tulyaganov, V. Vladislav, Kharton, A. Aleksey, Yaremchenko, M.F. José, Ferreira, The effect of Cr_2O_3 addition on crystallization and properties of La_2O_3-containing diopside glass–ceramics, Acta Mater. 56 (2008) 3065–3076.
[17] P. Saswati Ghosh, A. Kundu, R.N. Das Sharma, H.S. Basu, Maiti, Microstructure and property evaluation of barium aluminosilicate glass–ceramic sealant for anode-supported solid oxide fuel cell, J. Eur. Ceram. Soc. 28 (2008) 69–76.
[18] A.M. Efimov, Section 1. Optical properties of oxide glasses: quantitative IR spectroscopy: applications to studying glass structure and properties, J. Non-Cryst. Solids 203 (1996) 1–11.
[19] H. Darwish, M.M. Gomma, Effect of compositional changes on the structure and properties of alkali–alumino borosilicate glasses, J. Mater. Sci.: Mater. Electron. 17 (2006) 35–42.

[20] Yin Cheng, Hanning Xiao, Wenming Guo, Weiming Guo, Structure and crystallization kinetics of $PbO–B_2O_3$ glasses, Ceram. Int. 33 (2007) 1341–1347.
[21] A.K. Hassan, L. BÖrjesson, L.M. Torell, The boson peak in glass formers of in creasing fragility, J. Non-Cryst. Solids 172/174 (1994) 154–160.
[22] E.I. Kamitsos, A.P. Patsis, M.A. Karakassides, G.D. Chryssikos, Infrared reflectance spectra of lithium borate glasses, J. Non-Cryst. Solids 126 (1990) 52–67.
[23] E.I. Kamitsos, A.P. Patsis, G.D. Chryssikos, Infrared reflectance investigation of alkali diborate glasses, J. Non-Cryst. Solids 152 (1993) 246–257.
[24] S. Monika Arora, G. Baccaro, D. Sharma, K.S. Singh, D.P. Thind, Singh, Radiation effects on $PbO–Al_2O_3–B_2O_3–SiO_2$ glasses by FTIR spectroscopy, Nucl. Instrum. Methods B 267 (2009) 817–820.
[25] Longfei Zhou, Huixing Lin, Wei Chen, Lan Luo, IR and Raman investigation on the structure of $(100 - x)B_2O_{3-x}$ [0.5 BaO–0.5ZnO] glasses, J. Phys. Chem. Solids 69 (2008) 2499–2502.
[26] Yin Cheng, Hanning Xiao, Wenming Guo, Weiming Guo, Structure and crystallization kinetics of $Bi_2O_3–B_2O_3$ glasses, Thermochim. Acta 444 (2006) 173–178.
[27] S. Mahadevan, A. Giridhar, A.K. Singh, Calorimetric measurements on As–Sb–Se glasses, J. Non-Cryst. Solids 88 (1986) 11–34.
[28] A. Hruby, Evaluation of glass-forming tendency by means of DTA, Physica B 22 (1972) 1187–1193.
[29] A. Hruby, Glass-forming tendency in the GeSx system, Physica B 23 (1973) 1263–1272.
[30] C. Lara, M.J. Pascual, R. Keding, A. Durán, Electrical behaviour of glass–ceramics in the systems $RO–BaO–SiO_2$ (R = Mg, Zn) for sealing SOFCs, J. Power Sources 157 (2006) 377–384.